

Theoretical and Statistical Models for Predicting Flux in Direct Contact Membrane Distillation

Dahiru U. Lawal, Atia E. Khalifa

King Fahd University of Petroleum & Minerals Department of Mechanical Engineering Dhahran 31261 Saudi Arabia

ABSTRACT

Theoretical model has been applied to predict the performance of Direct Contact Membrane Distillation (DCMD) based on the analysis of heat and mass transfer through the membrane. The performance of DCMD on the account of different operating parameters had been predicted. Feed inlet temperature, coolant inlet temperature, feed flow rate and coolant flow rate are the considered performance variables. Based on the data obtained from theoretical model, statistical analysis of variance (ANOVA) was then performed to determine the significant effect of each operating factors on the DCMD system performance. A new regression model was subsequently developed for predicting the performance of the DCMD system. Results revealed that both theoretical and regression models were in good agreement with each other and also with the selected experimental data used for validation. The maximum percentage error between the two models was found to be 1.098%. Hence, the developed regression model is adequate for predict the performance of DCMD system within the domain of the considered analysis.

Keywords– Water Desalination, Direct contact membrane distillation, theoretical modelling, ANOVA, Taguchi methodology, regression model.

I. Introduction

Membrane distillation (MD) is a thermally driven separation process in which separation is achieved as a result of phase change. MD process is a technique for separating water vapour from a liquid saline aqueous solution by transport through the pores of hydrophobic membranes, where the driving force is the vapour pressure difference created by temperature difference across the membrane. MD has been applied to the separation of volatile compounds from aqueous mixtures, continuous removal of alcohol produced by fermentation, breaking of azeotropic mixtures, and concentrating various acids. Findley was the first to relate the separation techniques now known as membrane distillation [1]. MD differs from other membrane technology in that the driving force for desalination is due to the vapour pressure difference, rather than the total pressure of water across the membrane.

The four basic configurations mainly utilized in MD are the vacuum membrane distillation (VMD), direct contact membrane distillation (DCMD), sweeping gas membrane distillation (SGMD) and air gap membrane distillation (AGMD). In all these MD configuration, membrane coefficient (permeability) limit the performance of MD system.

In DCMD configuration, the temperature difference between the sides of a hydrophobic membrane material creates partial pressure difference which incites water molecule evaporated at the hot

feed side to permeate the pores of the membrane. The vaporized water then condensed in the flowing coolant solution.

Theoretical models had been developed and proposed by several researchers. L. Martinez and F.J. Florido Diaz [2] developed a model which is based on a dusty gas model of gas transport through porous media. A direct contact membrane distillation experiment was conducted using two flat sheet membrane material. Two experiment were carried out, in the first experiment, GVHP22 membrane was used while HVHP45 membrane material was employed in the second experiment. The output results show that the developed model prediction were in good agreement with the experimental results.

Jian-Mei Li et al [3] investigated experimentally in direct contact membrane distillation (DCMD and vacuum membrane distillation (VMD)), the influence of feed flow and feed temperature on permeate flux using an aqueous solution of 35g/l NaCl. Results revealed that for both DCMD and VMD, Polyethylene (PE) membrane material produces higher water flux in comparison to polypropylene (PP) membrane material.

Robert W Field et al [4] developed a model for overall mass transfer coefficient in direct contact membrane distillation. In the model developed, the membrane effective thickness is consider as the sum of the actual thickness. Results showed that the sum of the additional terms exceeds 100 μm , which implies that the flux is not inversely proportional to

membrane thickness. The study also revealed that the thermal efficiency does not depend on membrane thickness. In conclusion, the investigation revealed that the traditional method of combining Knudsen and the molecular diffusion coefficient overestimated the resistance. This leads to underestimation of flux.

Tzahi Y. Cath et al [5] experimentally investigate a new DCMD membrane module. In a turbulent flow regime and with a feed water temperature of only 40 °C, the performances of three hydrophobic micro porous membranes were evaluated. Result revealed that reduction in temperature polarization and permeability obstructions could be obtained simultaneously by careful design of a membrane module and configuration of the MD system. It was shown that the permeate flux obtained for the new approach is more than twice of the traditional mode of DCMD when operating at relatively low temperatures. Both NaCl and synthetic sea feed solutions were used in investigation. Economic aspects of the improved DCMD process was discussed and the new enhanced DCMD process was compared with the reverse osmosis (RO) process for desalination.

Design of Experiments (DOE) is a powerful statistical tool for process design and products formulation. It can be used to either quantitatively identify the right input parameter to produce a high quality product or enhance process performance. DOE has been successfully applied in the parametric study of AGMD.

Khayet and Cojocaru[6] modelled and optimized air gap membrane distillation system using response surface methodology. The specific performance index and performance index were predicted using developed regression model with the effect of energy consumption as function of different operating variables. Statistical analysis was performed using analysis of variance (ANOVA) to determine the significant level of each parameters. Using Monte Carlo simulation, an optimum variable combination for performance index were found to be 71°C feed inlet temperature, 13.9°C cooling inlet temperature and 183L/h feed flow rate. These variables combination gave an experimental permeate flux of 47.189 kg/m²h. The optimum variables combination for specific performance index were found to be 59°C feed inlet temperature, 13.9°C cooling inlet temperature and 205 L/h feed flow rate which resulted to an experimental output of 188.7kg/kWh.

The objective of this study is to compare the performance of mathematical model with that of developed statistical model in modelling DCMD system. The modelling results will be validated against the experimental data available. In statistical analysis, both the Taguchi methodology and regression analysis will be exploit to ascertain the

influence of DCMD operating parameters. Feed temperature, feed flow rate, coolant temperature, and coolant flow rate are the considered factors.

1.1 Taguchi Techniques

Taguchi method is a structured and robust design approach for determining best combination of factors to yield product. It is used to investigate how different parameters affect the mean and variance of a system performance. The most important stage in design of experiment lies in the selection of control factors. So, many factors are included at the initial stage, while non-significant factors are identified and eliminated at this earlier stage of experimental design [7]. The DOE using Taguchi technique can economically satisfy the needs of problem solving and system design optimization, as it allows fewer experimental runs usually leading to significant reduction in time and resources requirement for experimentation.

While Traditional Design of Experiments focuses on how different design factors affect mean results, Taguchi's DOE put emphasis on variation rather than the mean. Additionally, the former treats noise as an extraneous factor, while the latter considers it as a central point of its analysis. Toraj and Safavi[8] applied Taguchi techniques in the optimizing the performance of vacuum membrane distillation system for water desalination. In the study, feed temperature in the range of 35°C to 55°C, feed flow rate of 15–60 mL/s, vacuum pressure of 30–130 mbar and feed concentration of 50-150 g/L were investigated. Application of ANOVA showed that all the operating parameters were significant, with each having different level of importance. The optimum permeate flux reported was 16.96 kg/m²h at 55°C feed temperature, 30 mL/s feed flow rate, 50 g/L feed concentration and 30 mbar vacuum pressure.

II. Theory

The system considered in this study is as depicted in fig.1. It consists of feed chamber and coolant chamber separated by a hydrophobic membrane material. In this configuration, heat and mass transfer occurs simultaneously. The feed temperature (T_f) decrease over the feed side boundary layer to T_{mf} at the membrane surface. As part of feed solution evaporates and diffuses through membrane pores, heat is conducted through membrane to the coolant chamber. The coolant temperature (T_c) rises across the cold boundary layer to T_{mc} as vapour condenses into the fresh water [9]. The driving force is hence the vapour pressure difference between T_{mf} and T_{mc} , which is less than the vapour pressure difference between T_f and T_c . The process is otherwise called temperature polarization [10].

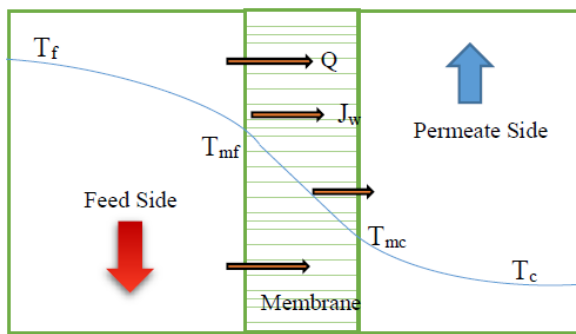


Fig. 1. Schematic diagram of heat and mass transfer across MD membrane [11].

2.1 Mass Transfer

Mass transfer in MD takes place by convection and diffusion of vapour through the micro porous membrane sheet [11, 12]. In DCMD, both heat and mass transfer process takes place through the membrane as shown in figure1. The water permeate flux (J_w) obtained depends on the membrane characteristic and the created driving force.

The mechanism of mass transfer in membrane pores is guided by three basic processes. Knudsen diffusion (K), Poiseuille (viscous) flow (P), Molecular diffusion (M) and transition model are the mechanism the mass transfer through the membrane pores. The general expression for mass transfer in MD is [11, 13]:

$$J_w = C_w \Delta P_m \quad (1)$$

Where C_w is the overall mass transfer coefficient which is the reciprocal of an overall mass transfer resistance and $\Delta P_m = P_{mf} - P_{mc}$ is the vapour pressure difference between the sides of the membrane sheet. Thus:

$$J_w = C_w (P_{mf} - P_{mc}) \quad (2)$$

For pure water, P_m can be estimated from Antoine equation [9];

$$P_m = \exp\left(23.328 - \frac{3841}{T_m - 45}\right) \quad (3)$$

Khayet et al [14] showed that the permeate flux has a linear relation with the partial pressure difference across the membrane pores as given in eq. (4) when the feed is water and when the temperature difference through the membrane is low.

$$P_{mf} - P_{mc} = \left(\frac{dP}{dT}\right)_{T_m} (T_{mf} - T_{mc}) \quad (4)$$

Substitution of eq. (4) into (2) results in:

$$J_w = C_w \left(\frac{dP}{dT}\right)_{T_m} (T_{mf} - T_{mc}) \quad (5)$$

Where P_{mf} and P_{mc} are the transmembrane vapour pressure at the feed and coolant sides respectively. T_{mf} and T_{mc} are the transmembrane temperature at the feed and permeate sides respectively. The term $\left(\frac{dP}{dT}\right)_{T_m}$ is obtained from the combination of Clausius–Clapeyron equation and the Antoine equation as given in [9]:

$$\left(\frac{dP}{dT}\right)_{T_m} = \frac{\Delta H_v}{RT_m^2} \exp\left(23.328 - \frac{3841}{T_m - 45}\right) \quad (6)$$

Where R is the gas constant, T_m is the mean temperature in kelvin given by $T_m = \frac{T_{mf} + T_{mc}}{2}$ and ΔH_v is the heat of vapourisation of water which is expressed as:

$$\Delta H_v = 1.7535T + 2024.3 \quad [\text{kJ/kg}] \quad (7)$$

2.2 Membrane Permeability (C_w)

Knudsen number (K_n) is the governing quantity which provides the guideline for identifying which type of mechanism of mass transfer dominates the flow under the given experimental condition just like how Reynolds number is used as a guide in defining if a flow is laminar, turbulent and transitional. Based on kinetic theory of gases, the mechanism of mass transfer through DCMD membrane must be by Knudsen model or ordinary molecular diffusion or poiseuille (viscous) flow model or a combination of these models.

Usually, viscous flow model neglected in DCMD because both feed and permeate solutions are maintained in direct contact with membrane material under atmospheric. The total pressure is constant at atmospheric leading to negligible viscous kind of flow [11, 12, 15, 16].

The expression for Knudsen number is given as:

$$K_n = \frac{\lambda_w}{d_p} \quad (8)$$

Where d_p is the membrane pore size and λ_w is the mean free path of the water molecule which may be estimated from:

$$\lambda_w = \frac{K_B T}{\sqrt{2} \pi P_m (2.641 \times 10^{-10})^2} \quad (9)$$

Where K_B is the Boltzmann constant, P_m is the mean pressure within the membrane pores, T is the absolute mean temperature in the pores (Kelvin).

When membrane pore size is low in comparison with mean free path of water molecules in vapour state ($d_p < 0.1 \lambda_w$), then the molecule-pore wall collisions preside over the molecule-molecule impact, so the Knudsen kind of flow is responsible

for the mechanism of mass transfer. The expression below provides membrane permeability (C_w) in Knudsen region [4, 9, 17, 18]:

$$C_w = \frac{2\pi}{3} \frac{1}{RT} \left(\frac{8RT}{\pi M_w} \right)^{1/2} \frac{r_k^3}{\tau \delta} \quad (10)$$

Where r_k is the membrane pore radius, τ is the membrane tortuosity, δ is the membrane thickness and M_w is the molecular mass of water.

When the mean free path of the transported water molecules in vapour state is less than the membrane pore size ($d_p > 100\lambda_w$), then the molecule-molecule collision is predominant over the molecule to pore wall, so ordinary molecular diffusion is responsible for the mass transfer in the continuum region. In this case, the below expression may be adopted to evaluate the membrane permeability [9, 18];

$$C_w^D = \frac{\pi}{RT} \frac{PD_w}{P_a} \frac{r_D^2}{\tau \delta} \quad (11)$$

Where P_a is the air pressure in the membrane, P is the total pressure inside the membrane pore and D_w is the diffusion coefficient which can be obtained from the following expressions [9, 19, 20, 21]:

$$PD_w = 1.895 \times 10^{-5} T^{2.072}$$

$$PD_w = 1.19 \times 10^{-4} T^{1.75} \quad (12)$$

$$PD_w = 4.46 \times 10^{-6} T^{2.334}$$

Where PD_w is in $\text{Pa} \cdot \text{m}^2/\text{s}$

Transition region mechanism occurs when we $0.1\lambda_w < d_p < 100\lambda_w$. In this case, the molecules of liquid water collides with each other and diffuses through the air molecules. For transition region, combined Knudsen-ordinary molecular diffusion type of flow is responsible for the mass transfer. The model for membrane permeability for transition region is expressed as [9, 18]:

$$C_w^C = \frac{\pi}{RT} \frac{1}{\tau \delta} \left[\left(\frac{2}{3} \left(\frac{8RT}{\pi M_w} \right)^{1/2} r_k^3 \right)^{-1} + \left(\frac{PD_w}{P_a} r_k^2 \right)^{-1} \right]^{-1} \quad (13)$$

Membrane tortuosity can be estimated using the correlation suggested by Macki[22]:

$$\tau = \frac{(2-\varepsilon)^2}{\varepsilon} \quad (14)$$

Where ε is the membrane porosity.

2.3 Heat Transfer

Heat transfer in (DCMD) involved three (3) major steps as depicted in fig. 1. The steps are:

i. Convection heat transfer in the feed boundary layer (Q_f) given by [9]:

$$Q_f = h_f(T_f - T_{mf}) \quad (15)$$

ii. Heat transfer across the membrane sheet (Q_m) is composed of latent heat of vaporization (Q_v) and conduction heat transfer through the membrane material and the gas filling pores (Q_c). This is given as [9]:

$$Q_m = Q_c + Q_v \quad (16)$$

Where

$$Q_v = J_w \Delta H_v = C_w \left(\frac{dP}{dT} \right)_{T_m} (T_{mf} - T_{mc}) \Delta H_v \quad (17)$$

And

$$Q_c = -K_m \frac{dT}{dX} = \frac{K_m}{\delta} (T_{mf} - T_{mc}) \quad (18)$$

Combining Eqs. (16), (17) and (18) leads to:

$$Q_m = \left(\frac{K_m}{\delta} + C_w \left(\frac{dP}{dT} \right)_{T_m} \Delta H_v \right) \Delta T_m \quad (19)$$

Where $\Delta T_m = T_{mf} - T_{mc}$

iii. Heat transfer in the coolant boundary layer (Q_p) expressed as:

$$Q_p = h_p(T_{mc} - T_c) \quad (20)$$

Different models has been employed in estimating thermal conductivity of the membrane material, but the following sets of equation is often used [9]:

$$K_m = \varepsilon K_g + (1 - \varepsilon) K_p \quad (21)$$

And the Isostress model [9, 20]:

$$K_m = \left[\frac{\varepsilon}{K_g} + \frac{(1-\varepsilon)}{K_p} \right]^{-1} \quad (22)$$

Where K_p And K_g are the thermal conductivity of the membrane material and that of the gas filling the membrane pores respectively.

At steady state, the overall heat transfer through the DCMD system is given by:

$$Q = Q_f + Q_m + Q_p \quad (23)$$

Combination and manipulation of Eqs (15) to (20) leads to:

$$T_{mf} = \frac{\frac{K_m}{\delta} \left(T_c + \frac{h_f}{h_p} T_f \right) + h_f T_f - J_w \Delta H_{vw}}{\frac{K_m}{\delta} + h_f \left(1 + \frac{K_m}{\delta h_p} \right)} \quad (24)$$

$$T_{mp} = \frac{\frac{K_m}{\delta} \left(T_f + \frac{h_p}{h_f} T_c \right) + h_p T_c + J_w \Delta H_{vw}}{\frac{K_m}{\delta} + h_p \left(1 + \frac{K_m}{\delta h_f} \right)} \quad (25)$$

Eq. 24 and eq. 25 are the required temperature in eq. 3 and eq. 5. The heat transfer coefficients (h_f and h_p) can be estimated from Nusselt number given as [17]:

$$Nu_i = \frac{h_i d_i}{k_i} \text{ where } i = f \text{ and } p \quad (26)$$

and k is the thermal conductivity of the fluid, d is the hydraulic diameter, h is the heat transfer coefficient and f is the feed and p is the permeate.

For laminar flow, the following empirical correlation can be used [22, 23]:

$$Nu = 1.86 \left(Re Pr \frac{d}{L} \right)^{0.33} \quad (27)$$

For turbulent flow, correlation below may be used [24]:

$$Nu = 0.023 Re^{0.8} Pr^{0.33} \left(\frac{\mu}{\mu_s} \right)^{0.14} \quad (28)$$

Where Pr and Re are the Prandtl and Reynolds numbers respectively and they are expressed as:

$$Pr = \frac{\mu C_p}{k}, \quad Re = \frac{\rho u d}{\mu} \quad (29)$$

where C_p , ρ , u , and μ are the specific heat capacity, density, average velocity and viscosity of the liquid respectively.

For feed solution containing dissolve salt, P_{mf} may be estimated using the Raoult's law expressed as [25]:

$$P_{mf} = (1 - CM_{Nacl}) P_m \quad (30)$$

Where, CM_{Nacl} is the molar solute concentration.

2.4 Simulation procedure

The solution to the above set of equations was implemented in Matlab. For flux prediction, an iterative method was adopted. Initially, guessed values were assigned for membrane surface temperatures (T_{mf} and T_{mc}). The guessed values are then used to calculate the permeate flux (J_w) as given in Eqs. (4) - (13), (27) and (28). The obtained flux (J_w) from these guess values is then utilized to calculate a corrected sets of membrane surface

temperatures. The above procedure is repeated until the difference between two consecutive iterations is less than 0.1%.

III. Results and Discussions

To examine the flux prediction capability of the theoretical model, its results were validated against the experimental work of Andrijesdottir et al [26]. The geometrical constants and the membrane properties used are tabulated in Table 1.

Table 1. Membrane Properties and Geometrical Constant Used [26]

Symbol	Values as used in [26]
δ	140 μ m
ϵ	0.88
Kg	0.029 W/mK
Kp	0.259 W/mK
d_p	0.20 μ m
R	8.314 J/Kmol
L	120 mm
W	104 mm
H	5.2 mm
A	$5.408 \times 10^{-4} \text{ m}^2$
d_h	$9.905 \times 10^{-3} \text{ m}$

The minimum and maximum temperature considered in the experimental work are 15°C and 60°C respectively and considering the membrane pore sizes of 2×10^{-7} as used in [26], it was confirmed by [11] that the best model for flux prediction in DCMD is the combined Knudsen-molecular diffusion kind of flow model. Hence the model to be adopted in this work.

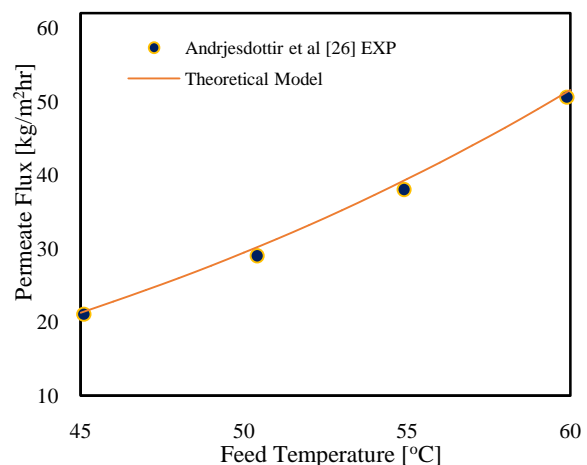


Fig. 2. Flux vs. feed temperature in DCMD for theoretical model and experiment [26]. Coolant temperature is kept at 21°C, feed flow rate is 12 L/min and coolant flow rate is 4 L/min.

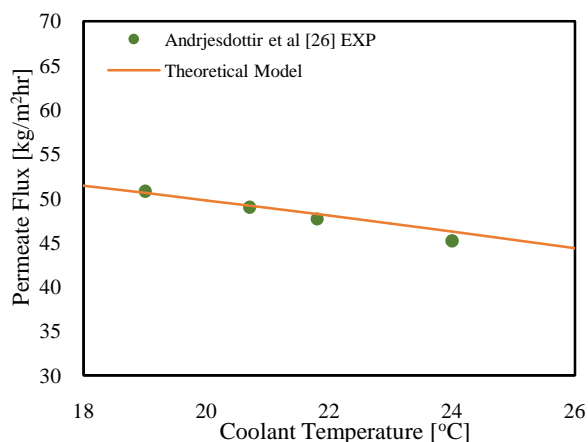


Fig. 3. Effect of coolant temperature on flux for theoretical model and experiment [26]. Feed temperature is kept at 60°C, feed flow rate is 12 L/min and coolant flow rate is 4 L/min.

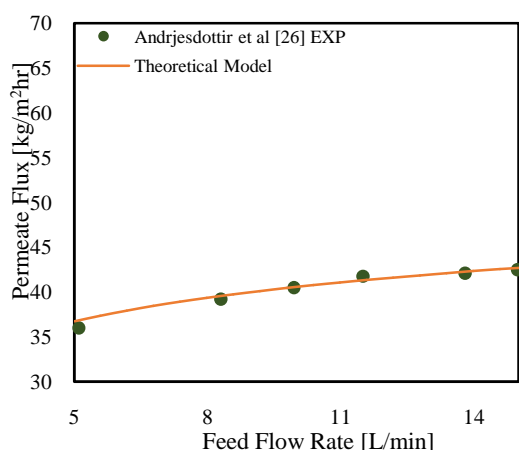


Fig. 4. Effect of flow rate on flux for theoretical model and experiment [26]. Coolant flow rate is 3 L/min, feed temperature is 60°C, and coolant temperature is 21°C.

Depicted in Figs. 2-4 are the results of flux prediction using combined Knudsen-molecular diffusion kind of flow model. The selected model was used to investigate the effect of feed inlet temperature, coolant inlet temperature and feed flow rate. In all the cases, results shows good agreement

between the model and the experiment with minimum percentage error of 0.00 % as obtained in Fig. 6 and maximum percentage deviation of 3.55 % as found in Fig. 4. Therefore, we are now save to employ the theoretical model in generating data for ANOVA and regression analysis which is our main objective in this study.

IV. Statistical Analysis

Statistical software MINITAB 16 was employed in the design and analysis of the datagenerated from the mathematical model. The five levels of parameters combination and the Taguchi $L_{25} (5^4)$ orthogonal arrays for this combinations are tabulated in Table 2. In total, 25theoretical data were generated and the results are as presented in Table 2.The main effect plots are as depicted in fig. 5. The plots are effectively used to investigate the trends and influence of each factor (operating parameters). It is obvious from Fig. 5 that the permeate flux increases with increasing feed temperature. This is in fact due to the exponential rise in water vapour pressure [9, 25, 27, 28].

The permeate flux also increases with increasing feed flow rate and coolant flow rate. This can be attributed to the high turbulent generated in the channels because of higher mixing effect. This can also due to the fact that rise in flux can also be a result of increase in heat transfer coefficient in boundary layer at both feed and coolant sides of membrane which leads to reduction in temperature polarization effect. Reduction in permeate flux was however observed when coolant temperature rises. The drop in permeate flux is caused by the decrease in driving temperature difference between the feed side and condensation surface. It is obvious from the mean effect plots that the feed inlet temperature has the most significant effect on the system performance in comparison to other operating parameters.

4.1 ANOVA

The experimental data were subjected to statistical scrutiny via analysis of variance (ANOVA). ANOVA was performed in order to observe the significant effect of each operating parameters. The analysis was conducted at 95% confidence level (level of significant $\alpha = 0.05$). The obtained ANOVA results are tabulated in Table 3. It can be noticed that each factors has P-value less than the chosen confidence level (0.05). This is an indication that each operating factors are statistically significant. As such, we reject null hypothesis and accept alternative hypothesis.

However, it can be observed from Table 3 that feed temperature provides the most significant effect on the DCMD performance having P-value of 0.000. Next to feed temperature in level of significant effect on the system flux is the coolant temperature with P-value of 0.017, then the feed flow rate having P-value of 0.032. Coolant flow rate provides the least significant effect on permeate flux and its P-value is 0.04

Table 2: Taguchi L₂₅ (5⁴) orthogonal design matrix and DCMD responses.

Runs	Feed Temperature [°C]	Coolant Temperature [°C]	Feed Flow rate [L/min]	Coolant Flow rate [L/min]	Responses		Percentage Error [%]
					Theoretical Model [kg/m ² h]	Regression Model [kg/m ² h]	
1	40	10	2	1	14.5076604	14.376604	0.91159498
2	40	15	4	3	15.6692742	15.582742	0.55530792
3	40	20	6	5	16.889888	16.78888	0.60163632
4	40	25	8	7	17.7995018	17.995018	1.09843636
5	40	30	10	9	19.2550115	19.201156	0.28048082
6	50	10	4	5	31.471427	31.41427	0.18194598
7	50	15	6	7	32.820408	32.620408	0.61311312
8	50	20	8	9	33.8299654	33.826546	0.01010881
9	50	25	10	1	25.874244	25.774244	0.38798422
10	50	30	2	3	15.420182	15.520182	0.64850078
11	60	10	6	9	58.2285896	58.156836	0.12337962
12	60	15	8	1	50.304534	50.104534	0.39916547
13	60	20	10	3	51.110672	51.310672	0.39130771
14	60	25	2	5	41.305661	41.05661	0.60660391
15	60	30	4	7	42.2062748	42.262748	0.13380285
16	70	10	8	3	85.145862	85.345862	0.23489104
17	70	15	10	5	86.023552	86.552	0.61430618
18	70	20	2	7	76.097938	76.297938	0.26281921
19	70	25	4	9	77.1034040	77.504076	0.5196553
20	70	30	6	1	69.651774	69.451774	0.28796961
21	80	10	10	7	131.549822	131.498228	0.03923612
22	80	15	2	9	120.401416	121.244166	0.69994974
23	80	20	4	1	112.500161	113.191864	0.61484546
24	80	25	6	3	113.98002	114.398002	0.36671515
25	80	30	8	5	115.95414	115.60414	0.30275732

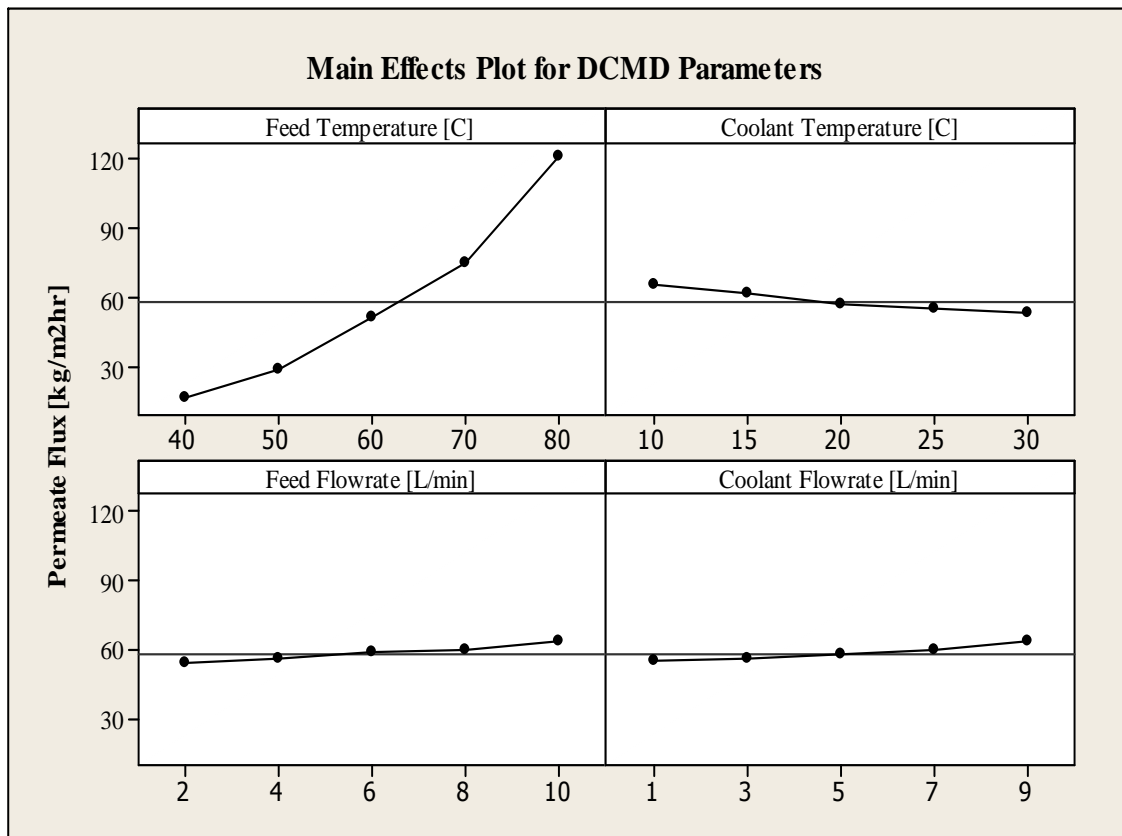


Figure 5: Main effect plot of the permeate flux

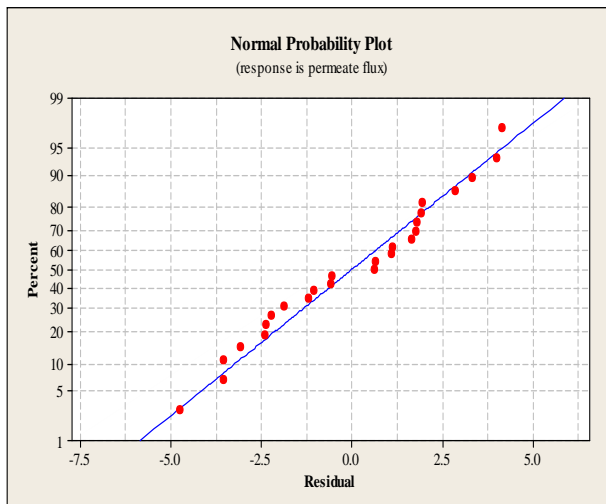


Figure 6: Normal probability plot

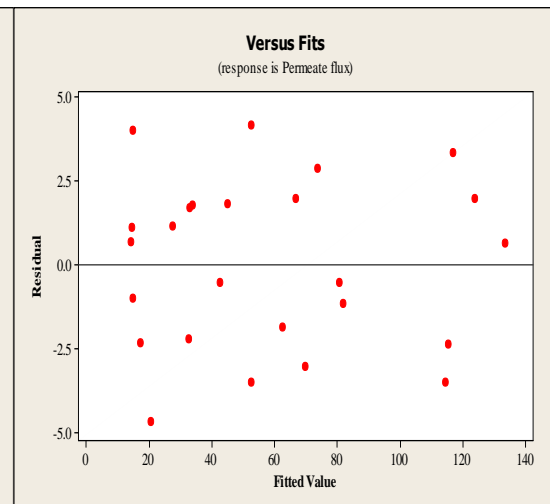


Figure 7: Residuals vs fits plot

Table 3: Analysis of variance for responses, using adjusted SS for tests

Source	DF	Seq SS	Adj SS	Adj MS	F	P
Feed Temperature [C]	4	34568.9	34568.9	8642.23	453.32	0.000
Coolant Temperature [C]	4	448.5	448.5	112.13	5.88	0.017
Feed Flow rate [L/min]	4	267.2	267.2	66.79	3.50	0.032
Coolant Flow rate [L/min]	4	184.3	184.3	46.07	2.42	0.048
Residual Error	8	152.5	152.5	19.06		
Total	24	35621.4				

Fig. 6 displays normality plots of residuals. It was observed that the theoretical data point either passes through the mean line (fitted line) or clusters around it. This is an indication that neither normality assumption was violated nor any evidence pointing to possible outliers. As such, we conclude that normal distribution is an approximate model for the system performance. Thus, the mean data generated is normally distributed along the fitted line. Fig. 7 depicts the residuals against fitted values. The tendency to have runs of positive and negative residuals indicates positive correlation which validates independence assumption. It is obvious from fig. 7 that no recognized pattern exist. This implies that the constant variance assumption holds.

4.2 Regression Modelling

In model generation, permeate flux was modeled as dependent variable while the feed temperature, coolant temperature, feed flow rate and coolant flow rate as independent variables.

Prior to model generation, the actual response surface was plotted in order to have the general idea of the suitable variables function that will enable the smooth fitting of the model to the actual response surface. Following which potential suitable models were generated, first, with feed temperature, coolant temperature and feed flow rate as variables. Thereafter, all other possible suitable combinations were generated, including quadratic terms depending on the shape of the actual response plane. Comparisons were then made and the best model to represent the property change was selected based on the adjusted correlation coefficient value (R^2 (adj)) and standard error of estimate (S) of each model.

Thus, the best subsets regression approach was adopted during model generation. In this approach, all possible regression equations were estimated using all possible combinations of independent variables. The best fit of the model was selected based on the highest adjusted R-square and lowest standard error estimate

(S). Thus, the best regression model for predicting permeates flux is given by:

$$Y = 69.9139 - 3.26298A + 0.0485245A^2 - 0.587518B + 1.14602C + 0.925844D(31)$$

Where Y is the predicted permeate flux [$\text{kg/m}^2\text{h}$], A is the Feed temperature [$^{\circ}\text{C}$], B is the Coolant Temperature [$^{\circ}\text{C}$], C is the Feed flow rate [L/min] and D is the coolant flow rate [L/min].

It can be observed from Table 4 that the regression model is significant with P-Value of 0.0000000. The generated model has R-Square of 99.04%, meaning that 99.04% of variation in permeate flux is captured by variation in feed temperature, coolant temperature, feed flow rate and coolant flow rate. The model also has adjusted R-Sq of 98.79%, signifying that 98.79% of variation in permeate flux is explained by variation in feed temperature, coolant temperature, feed flow rate and coolant flow rate, taking into account the theoretical data size and number of independent variables.

The model also has a standard error estimate (S) of 4.23340 and (S) is the measure of variation of observed permeate flux (J) from the regression line. It is worth noting that the magnitude of S is judged based on the relative size of the system performance values in the theoretical data. The general conclusion is that; the lower the S value, the better the generated model.

Analysing the terms in the regression equation, the highest positive main effect is contributed by feed inlet temperature (variable A in Eq. 31). While the feed inlet temperature has a linear negative main effect on the flux, its quadratic positive term (A^2) overrun the negative effect of the linear term. Hence increasing this term (A) led to tremendous increases in permeate flux. The maximum negative main effect is attributed to the cooling inlet temperature (variable B in Eq. 31), meaning that increasing this term will result in reduction in the permeate flux.

Table 4: Analysis of variance for responses, using adjusted SS for tests

Source	DF	Seq SS	Adj SS	Adj MS	F	P
Regression	5	35280.9	35280.9	7056.18	393.723	0.0000000
A	1	32767.1	512.6	512.58	28.601	0.0000368
B	1	431.5	431.5	431.47	24.075	0.0000980
C	1	262.7	262.7	262.67	14.657	0.0011338
D	1	171.4	171.4	171.44	9.566	0.0059894
A (SQR)	1	1648.2	1648.2	1648.24	91.969	0.0000000
Error	19	340.5	340.5	17.92		

S = 4.23340

R-Sq = 99.04%

R-Sq(adj) = 98.79%

Both feed and coolant inlet flow rate (variables C and D respectively in Eq. 31) each has little positive main effect on DCMD system performance. This is an indication that increasing these terms will result in small increment in system performance.

4.3 Regression Model Validation

The generated regression model was subsequently used to predict permeate flux. Comparison was made between the prediction of regression model and theoretical model. The outcomes were then tabulated in Table 2. It can be observed from Table 2 that both regression model results and that of theoretical model were in good agreement with the maximum percentage error of 1.098%.

Effort was also made to validate the regression model against the experimental data of Andrijsdottir et al [26] as depicted in fig. 8-10. For the effect of feed inlet temperature, the maximum percentage error recorded was 2.98% and that of coolant temperature was found to be 0.49%, while that of feed flow rate happened to be 1.68%. The prediction of this close accuracy to the experimental data is an indication that the developed regression model has the capacity to adequately predict DCMD permeate flux. Hence, based on statistical analysis, the developed model is considered suitable for predicting DCMD system performance within the domain of theoretical inputs.

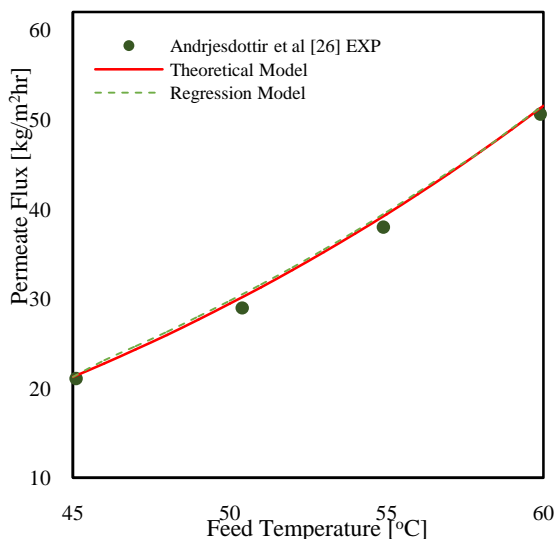


Fig. 8. Flux vs. feed temperature in DCMD for the models and experiment [26]. Coolant temperature is kept at 21°C, feed flow rate is 12 L/min and coolant flow rate is 4 L/min.

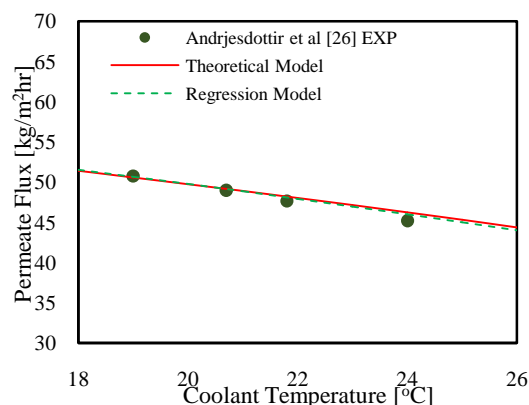


Fig. 9. Effect of coolant temperature on flux for the models and experiment [26]. Feed temperature is kept at 60°C, feed flow rate is 12 L/min and coolant flow rate is 4 L/min.

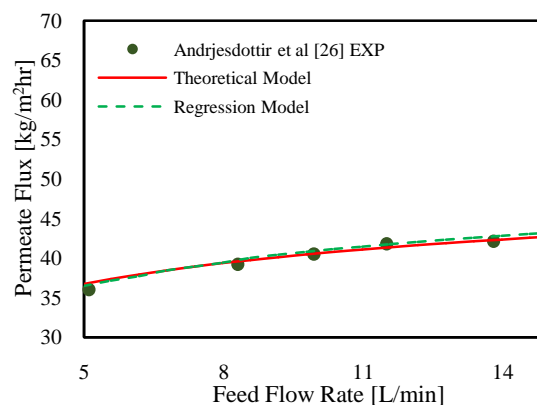


Fig. 10. Effect of flow rate on flux for the models and experiment [26]. Coolant flow rate is 3 L/min, feed temperature is 60°C, and coolant temperature is 21°C.

V. Conclusion

The basic concepts of heat and mass transfer analysis had been performed to portray the effect operating parameters on DCMD system performance. Taguchi method and applied regression were employed to model DCMD system for water desalination. Both the theoretical and regression models were tested on the effect feed temperature, feed flow rate coolant temperature and coolant flow rate. Results are validated against the experimental work of Andrijsdottir et al [26]. Theoretical model prediction showed a good match with the experimental results used for validation. For the regression equation, the maximum overall positive effect is attributed to feed inlet temperature and the highest negative main effect is observed from coolant inlet temperature. Both feed and coolant flow rates have little main effect on DCMD system performance.

VI. Acknowledgment

The authors would like to thank King Fahd University of Petroleum & Minerals (KFUPM) for providing all the necessary support needed in this work under the funded project # IN121043.

References

- [1] A.S. Jonsson, R. Wimmerstedt, and A.-C. Harrysson, *Membrane distillation-A theoretical study of evap. through microporous membranes*, *Desalination*, vol. 56, pp. 1985, 237-249.
- [2] L. Martínez, and F.J. Florido-Díaz, *Theoretical and experimental studies on desalination using membrane distillation*, *Desalination*, vol.139(1-3),2001,pp. 373-379.
- [3] J. M. Li, Z. K. Xu, Z. M. Liu, W. F. Yuan, H. Xiang, S. Y. Wang, Y. Y. Xu, *Microporous polypropylene and polyethylene hollow fiber membranes. Part 3. Experimental studies on membrane distillation for desalination*, *Desalination*, vol. 155(2), 2003, pp. 153-156.
- [4] R.W. Field, H.Y. Wu, J. J. Wu, *Multiscale Modeling of Membrane Distillation: Some Theoretical Considerations*, *Industrial & Engineering Chemistry Research*, vol. 52 (26), 2013, pp. 8822-8828.
- [5] T. Y. Cath, V.D. Adams, A.E. Childress, *Experimental study of desalination using direct contact membrane distillation: a new approach to flux enhancement*, *Journal of Membrane Science*, vol. 228(1), 2004, pp. 5-16.
- [6] M. Khayet, C. Cojocaru, *Air gap membrane distillation: Desalination, modeling and optimization*, *Desalination* 287, 2012, 138-145.
- [7] S. S. Madaeni, S. Koocheiki, *Application of Taguchi method in the optimization of wastewater treatment using spiral-wound reverse osmosis element*, *Chemical Engineering Journal* 119, 2006, 37-44.
- [8] M. Toraj, M. A. Safavi, *Application of Taguchi method in optimization of desalination by vacuum membrane distillation*, *Desalination* 249: 2009, 83-89.
- [9] M. Khayet, T. Matsuura, *Membrane distillation principles and applications*, (Elsevier B.V. 2011, ch. 10, pp. 254-268).
- [10] L. M. Camacho, L. Dumeé, J. Zhang, J. li, M. Duke, J. Gomez, S. Gray, *Advances in Membrane Distillation for Water Desalination and Purification Application*, *Water*, vol. 5, 2013, p. 94-196.
- [11] U. L. Dahiru, E. A. Khalifa, *Flux prediction in Direct contact membrane distillation*, *International Journal of Materials, Mechanics and Manufacturing*, vol.2, No. 4 2013..
- [12] R.W. Schofield, A.G. Fane, C.J.D. Fell, *Heat and mass transfer in membrane distillation*, *Journal of Membrane Science*, vol.33, 1987, pp. 299-313.
- [13] J. Zang, N. Dow, M. Duke, E. Ostarcevic, J. D. Li, S. Gray, *Identification of material and physical features of membrane Distillation*, *Membrane for high performance desalination*, *Journal of Membrane Science*, vol. 349, 2010, pp. 295-303.
- [14] M. Khayet, P. Godino, J. I. Mengual, *Study of asymmetric polarization in direct contact membrane distillation*, *Separation Science and Technology*, vol. 39, 2005, pp. 125-147.
- [15] R.W. Schofield, A.G. Fane, C.J.D. Fell, *Factors affecting flux in membrane distillation*, *Desalination*, vol. 77, 1990, pp. 279-294.
- [16] R.W. Schofield, A.G. Fane, C.J.D. Fell, *Gas and vapour transport through micro porous membranes. II. Membrane distillation*, *Journal of Membrane Science*, vol. 53 (1-2), 1990, pp. 173-185.
- [17] A. Alkudhiri, N. Darwish, N. Hilal, *Membrane distillation: A comprehensive review*, *Desalination*, vol.287, 2012, pp.2-18.
- [18] M. Khayet, A. Velázquez, J.I. Mengual, *Modelling mass transport through a porous partition: effect of pore size distribution*, *Journal of Non-Equilibrium Thermodynamics*, vol. 29 (3), 2004, pp. 279-299.
- [19] R.W. Schofield, A.G. Fane, C.J.D. Fell, *Gas and vapour transport through micro porous membrane I. Knudsen-Poiseuille transition*, *Journal of Membrane Science*, vol. 53 (1-2), 1990, pp. 159-171.
- [20] J. Phattaranawik, R. Jiratananon, A.G.Fane, *Effect of pore size distribution and air flux on mass transport in direct contact membrane distillation*, *Journal of Membrane Science*, vol. 215, 2003, pp. 75-85.
- [21] Y. Yun, R. Ma, W. Zhang, A. G. Fane, J. Li, *Direct contact membrane distillation mechanism for high concentration NaCl solutions*, *Desalination*, vol. 188, 2005, pp. 251-262.
- [22] S. Srisurichan, R. Jiratananon, A.G. Fane, *Mass transfer mechanisms and transport resistances in direct contact membrane*

- distillation process, *Journal of Membrane Science*, vol. 277 (1–2), 2006, pp. 186–194.
- [23] L. Martínez-Díez, M. I. Vázquez-González, *Temperature and concentration polarization in membrane distillation of aqueous salt solutions*, *Journal of Membrane Science*, vol. 156 (2), 1999, pp. 265–273.
- [24] K.W. Lawson, D.R. Lloyd, *Membrane distillation*, *Journal of Membrane Science*, vol. 124 (1), 1997, pp. 1–25.
- [25] M.N.A. Hawlader, R. Bahar, K. C. Ng, L. J. W. Stanley, *Transport analysis of an air gap membrane distillation (AGMD) process*, *Desalination & Water Treatment*, vol. 42, 2012, pp. 333–346.
- [26] O. Andrjesdottir, C. L. Ong, M. Nabavi, S. Paredes, A.S.G. Khalil, B. Michel, D. Poulikakos, *An experimentally optimized model for heat and mass transfer in direct contact membrane distillation*, *International Journal of Heat and Mass Transfer*, vol. 66, 2013, pp. 855–867.
- [27] F. A. Banat, J. Simandl, *Membrane distillation for dilute ethanol: Separation from aqueous streams*, *Journal of Membrane Science* 163: 1999, 333-348.
- [28] M. A. Izquierdo-Gil, M. C. Garcia-Payo, C. F. Pineda, *Air gap membrane distillation of sucrose aqueous solutions*, *J. Membr. Sci.* 155: 1999, 291-307.

Nomenclature

A	Cross sectional area [m ²]
d _p	Pore size [μm]
d _h	Hydraulic diameter [m]
D	Diffusion coefficient [m ² /s]
h	Heat transfer coefficient [W/m ² K]
H _v	Heat of vapourisation [kJ/kg]
J _w	Permeate flux [kg/m ² hr]
K	Thermal conductivity [W/mK]

C _w	Mass transfer coefficient [kg/m ² sPa]
K _m	Membrane thermal conductivity [W/mK]
K _g	Thermal conductivity of gas filling the pores [W/mK]
K _p	Thermal conductivity of membrane material [W/mK]
K _n	Knudsen number [dimensionless number]
M _w	Molecular weight [g/mol]
Nu	Nusselt Number [dimensionless number]
P	Total pressure [Pa]
P _m	Mean Pressure [Pa]
Pr	Prandtl Number [dimensionless number]
Q _s	Sensible heat transfer [W/m ²]
Q _v	Latent heat transfer [W/m ²]
Q _c	Conduction heat transfer [W/m ²]
R	Gas constant [J/Kmol]
Re	Reynolds number [dimensionless number]
Sc	Schmidt number [dimensionless number]
Sh	Sherwood number [dimensionless number]
T	Absolute temperature [K]

Subscripts and Superscripts

f	Feed
p	Permeate
m	Membrane
b	Bulk
mf	Feed side of membrane
mp	Coolant side of membrane
f	Bulk feed
c	Bulk permeate
s	surface

Greek Letters

δ	Membrane thickness; film thickness [μm]
ε	Porosity [%]
τ	Tortuosity [No unit]
μ	Viscosity [Ns/m ²]
λ	Mean free path [m]
ν	kinematic viscosity [m ² /s]
ρ	Density [kg/m ³]